DOI: 10.1002/ejic.201000228

Two Cobalt Compounds Based on Azide/Methoxy and Isonicotinate *N*-Oxide Ligands Exhibiting Ferromagnetic and Antiferromagnetic Interactions

Fu-Chen Liu,*[a] Min Xue,[a] Hai-Chao Wang,[a] and Jie Ou-Yang*[a]

Keywords: O ligands / Azides / Cobalt / Magnetic properties / Structure elucidation

Two new Co^{II} complexes, $[Co(OCH_3)L]$ (**1**) and $[Co_3(N_3)_4(OCH_3)_2L_2]$ (**2**) (L = isonicotinate *N*-oxide), were synthesized by solvothermal reaction and magnetically characterized. The cobalt ions in **1** and **2** all exhibit distorted octahedral coordination geometry. In **1**, there is a μ_{11}-methoxy/*syn*,*syn*-carboxylate mixed coordinated cobalt chain with mixed coordination, and a 3D structure is formed by the chains linked through the L ligands. In **2**, the alternating Co^{II} chains that are formed by linking the double end-on azide-bridged trimers are connected by the L ligands to form a 2D layer. Magnetic studies revealed that ferromagnetic coupling exists between the Co^{II} ions in **1**, and **1** undergoes a ferromagnetic transition at 2.5 K, whereas alternating ferromagnetic (FM) and antiferromagnetic (AFM) interactions exist in the chain of **2**.

Introduction

In recent years, considerable attention has focused on cobalt-based complexes because of their various coordination geometries, polychromatic colors, and particular significance in magnetochemistry.[1] The colors are associated with the coordination geometry; most commonly a light pink color occurs with octahedral coordination and a deep blue with tetrahedral coordination.[2] However, the coordination geometry is purely a consequence of serendipity and cannot be designed.[1,3] The remarkable character of the high-spin Co^{II} ion in octahedral geometry is the magnetic anisotropy originating from the unquenching of the orbital moment.[4] This results in variable magnetic behavior and complicated magnetostructural relationships in contrast to those of nickel, copper, and manganese complexes. Various bridges were studied between the high-spin Co^{II} complexes with d^7–d^7 exchange. The nature of the exchange depends on the conformation of the ligands. Among the numerous bridges that can mediate magnetic coupling effectively, carboxylate ligands were widely used. Generally, carboxylate ligands mediate antiferromagnetic coupling in the *syn,syn* and *anti*,*anti* modes and weak ferromagnetic (FM) or antiferromagnetic (AFM) coupling in the *syn*,*anti* mode.[5] The magnetic couplings transferred by other bridges, such as hydroxido or carboxylate-oxido and end-on azide, are governed by the angle between the bridging atom and the metal ions.[6] In multibridge complexes, the compensation and countercompensation effects have to be taken into account.[7] The design and arrangement of molecules in the solid state proceeds as expected. However, the design of molecules in the solid state is just an expectation; the true arrangement cannot be guessed beforehand. More fundamental research is required in order to understand the assembly process and magnetic behavior of these materials.

Herein, we report two new Co^{II} complexes, $[Co(OCH_3)L]_n$ (**1**) and $[Co_3(N_3)_4(HOCH_3)_2L_2]_n$ (**2**), where L is isonicotinate *N*-oxide. For the L ligand, replacement of the nitrogen donor site with an oxygen atom increases the flexibility and enriches the coordination modes of the ligand.[8] The L ligand in both complexes adopts the μ_4 bridging mode with *syn*,*syn*-carboxylate and μ_2-*N*-oxide groups, and the structure of the complexes depends on the short bridges used. Complex **1** is a brown-colored 3D complex based on a methoxy, carboxylate, and *N*-oxide mixed-bridged uniform Co^{II} chain. Complex **2** is mauve with a 2D layer structure consisting of double end-on azido-bridged trinuclear Co^{II} units. Magnetic studies indicate that dominant ferromagnetic coupling exists in **1** and that **1** exhibits the spin glass state at low temperature. The ferromagnetic trinuclear units in **2** are antiferromagnetically coupled, which leads to an antiferromagnetic ground state.

Results and Discussion

Description of Crystal Structures

Single-crystal X-ray diffraction analysis of brown crystals of **1** revealed a 3D coordination network crystallizing in the space group *Pnma*. The asymmetric unit contains half a Co^{II} ion, half an L ligand, and half a deprotonated methanol. Co1 is coordinated to six oxygen atoms of the two methoxy anions, the two *N*-oxide groups, and the two carboxylate groups of the four L ligands (Figure 1a). The

[a] School of Chemistry and Chemical Engineering, Tianjin University of Technology,
Tianjin 300384, P. R. China
E-mail: fuchenliutj@yahoo.com
ouyang@tjut.edu.cn

Supporting information for this article is available on the WWW under http://dx.doi.org/10.1002/ejic.201000228.

Table 1. Selected bond lengths (in Å) and angles (in °) for complexes **1** and **2**.

1			
Co1–O4#1	2.016(2)	Co1–O3#2	2.233(2)
Co1–O4	2.016(2)	Co1–O3#3	2.233(2)
Co1–O1#1	2.095(2)	Co1#4–O3–Co1#5	89.36(12)
Co1–O1	2.095(2)	Co1–O4–Co1#6	102.33(15)
#1 $-x, -y + 2, -z + 1$ #2 $x - 1/2, y, -z + 1/2$ #3 $-x + 1/2, -y + 2, z + 1/2$ #5 $x + 1/2, -y + 5/2, -z + 1/2$ #6 $-x, y - 1/2, -z + 1$			
2			
Co1–N1	2.090(8)	Co2–N1	2.094(9)
Co1–N1#1	2.090(8)	Co2–N4	2.123(7)
Co1–O1#2	2.127(6)	Co2–O4	2.135(7)
Co1–O1#3	2.127(6)	Co2–O3#4	2.169(6)
Co1–N4#1	2.200(8)		
Co1–N4	2.200(8)	Co2–O3–Co2#4	106.2(2)
Co2–O2#2	2.027(6)	Co2–N4–Co1	92.2(3)
Co2–O3	2.071(6)	Co1–N1–Co2	96.3(4)
#1 $-x, -y, -z - 1$ #2 $x - 1, y - 1, z - 1$ #3 $-x + 1, -y + 1, -z$ #4 $-x, -y, -z$			

bond lengths range from 2.016(2) to 2.233(2) Å (Table 1). The methoxy ligand adopts the μ_2 coordination mode when bridging two Co^{II} ions and has a Co1–O4–Co1C bond angle of 102.33(15)°. The L ligand bridges four Co^{II} ions through the *syn,syn*-carboxylate group and the μ_2-oxygen atom of the *N*-oxide group. The bond angle Co1–O3B–Co1A is 89.40(12)°. Thus a methoxy, *syn,syn*-carboxylate, and *N*-oxide mixed-bridged uniform Co^{II} chain is formed (Figure 2a). The distance between the neighboring Co^{II} ions in the Co1···Co1A chain is approximately 3.140 Å. Each chain connects four neighbors through the L ligands to give a 3D network (Figure 3a).

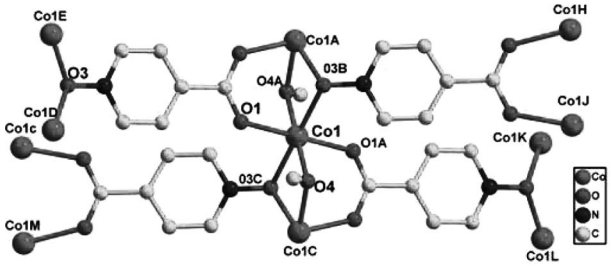

(a)

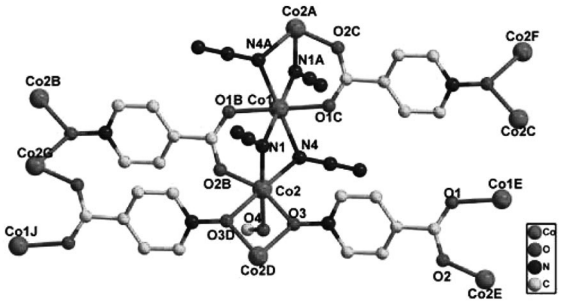

(b)

Figure 1. Coordination and linkage modes of the ligands and Co^{II} ions: (a) for **1** and (b) for **2**.

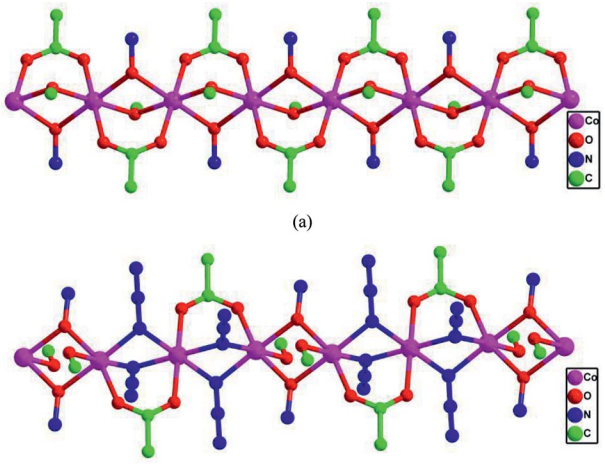

(a)

(b)

Figure 2. (a) *N*-Oxide/carboxylate/methoxy mixed-bridged Co^{II} linear chain in **1**. (b) Azide/*N*-oxide/carboxylate mixed-bridged Co^{II} linear chain in **2**.

In contrast, complex **2** has a 2D layer structure crystallizing in the space group $P\bar{1}$. The asymmetric unit contains one and a half Co^{II} ions, one L ligand, two azide anions, and one coordinated methanol. Co1 is located at the inversion center and is coordinated to four nitrogen atoms from azide anions and two oxygen atoms from two carboxylate groups. The bond lengths range from 2.090(8) to 2.200(8) Å (Table 1). Co2 has a distorted octahedral geometry and is coordinated to two nitrogen atoms from two azide anions and four oxygen atoms from the coordinated methanol, two *N*-oxide groups, and one carboxylate group from the three L ligands. The bond lengths range from 2.027(6) to 2.169(6) Å (Figure 1b). The methanol coordinates to Co2 in monodentate mode. The two azide anions both adopt the end-on mode, bridging two Co^{II} ions, thus a double end-on azido-bridged trinuclear Co^{II} unit is formed, which is favored by the carboxylate in *syn,syn* mode. The oxygen atoms of the *N*-oxide group adopt the μ_2 coordination

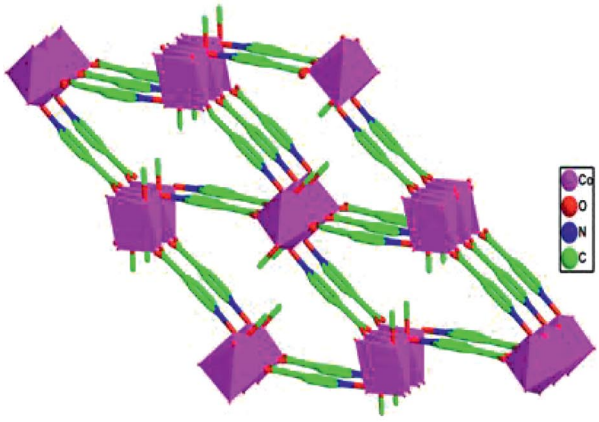

(a)

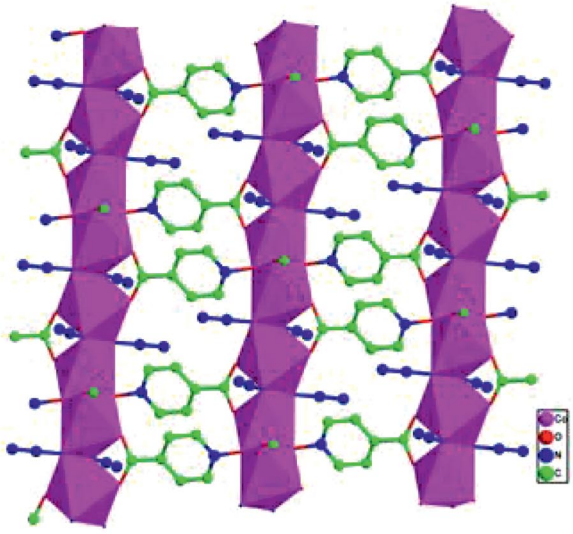

(b)

Figure 3. (a) Polyhedral view of the 3D structure of **1**. (b) Polyhedral view of the 2D structure of **2**.

mode when bridging two Co2 in neighboring trinuclear units. The trinuclear units are then linked together by the double *N*-oxide groups to give a Co^{II} chain (Figure 2b). The 2D layer structure of **2** can be described as 1D chains linked together by L ligands.

Magnetic Studies

Magnetic measurements have been carried out on crystalline samples of complexes **1** and **2**, which were are all pure as confirmed by X-ray powder diffraction (XRPD) (Figure S1). The magnetic susceptibilities of **1**, measured in the 2–300 K temperature range under 2 kOe and 1 kOe, are shown as $\chi_m T$ vs. T plots in Figure 4a. At 2 kOe $\chi_m T$ decreases slightly with the decrease in temperature down to 50 K (Figure S2). On further cooling, $\chi_m T$ increases sharply to a maximum of 11.89 $cm^3 K mol^{-1}$ at 3 K before dropping once again. Using the Curie–Weiss law to fit the data between 30 and 300 K gives C = 3.21 $cm^3 K mol^{-1}$ and θ = –1.99 K (Figure 4a). The C value is consistent with the value (2.5–3.4 $cm^3 K mol^{-1}$) of one non-interacting Co^{II} ion with spin–orbit coupling given g = 2.3–2.7. Generally, the Weiss constant of an isolated Co^{II} ion is about –20 K.[9] The small negative value of θ and the initial decrease in $\chi_m T$ can be attributed to the synergistic effect of the overall ferromagnetic coupling between the Co^{II} ions and the spin–orbit coupling of the octahedral Co^{II} ions. The $\chi_m T$ curve at 1 kOe is similar to that at 2 kOe but has a maximum at 19.48 $cm^3 K mol^{-1}$. The field-dependent maximum of the $\chi_m T$ curve indicates ferromagnetic order of the complex. Given the spin–orbit coupling due to the $^4T_{1g}$ ground state of the distorted octahedral Co^{II} complexes, exact calculations for deriving the J parameter from experimental data in the entire temperature range are only possible through sophisticated computer programs.[10] More recently, the exponential equation $\chi_m T = C_1 \exp(aJ/T) + C_2 \exp(\beta J/T)$ was used to estimate the strength of the magnetic exchange interactions of low-dimensional systems, in which $C_1 + C_2$ is

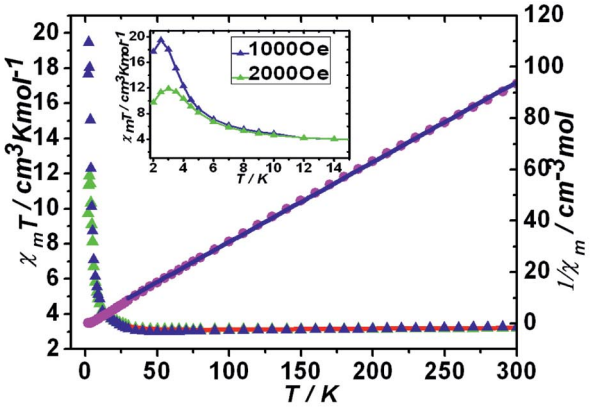

(a)

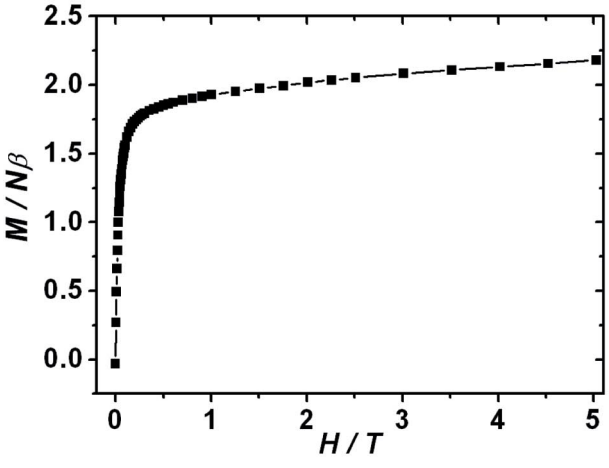

(b)

Figure 4. (a) Thermal variation of $\chi_m T$ and Curie plot for **1**. The solid line represents the best fit for the data where red is the exponential fit and blue is the fit to the Curie–Weiss equation. Inset: the thermal variation of $\chi_m T$ and Curie plot for **1** between 2–15 K. (b) Magnetization for **1** at 2 K.

equal to the Curie constant and αJ and βJ represent the "activation energies" corresponding to the magnetic exchange interaction.[11] Complex **1** is a quasi-isolated 1D chain from a magnetic perspective, because the linkage between the chains is only through the long bridging ligand L, which can only create a very small, almost negligible, magnetic coupling. With this assumption, it is possible to fit the experimental magnetic data by using the above-mentioned formula. Fitting the data in the 16–300 K range by using the exponential formula results in C_1 = 0.59 $cm^3 K mol^{-1}$, C_2 = 2.73 $cm^3 K mol^{-1}$, αJ = –98.47 K, and βJ = 5.74 K. The value of $C_1 + C_2$ is 3.32 $cm^3 K mol^{-1}$, which agrees with the Curie constant.[11] It is worth noting that the negative value for αJ does not, however, correspond to AFM behavior but to the spin–orbit coupling for octahedral Co^{II}.[11] The βJ value is the approximate magnitude of the ferromagnetic interactions for the chain.

The isothermal field-dependent magnetizations, $M(H)$, at 2 K at fields up to 5 T (Figure 4b) were measured for **1**. The field dependence of the magnetization does not follow a Brillouin curve. As shown in Figure 4b, the curves rise first sharply till saturation and then gradually to 2.2 $N\beta$ at 5 T for **1**. These findings are in agreement with those for one Co^{II} ion with S = 1/2 and g = 13/3.[12] The sharp increase of the $\chi_m T$ values at low temperature and the rapid saturation of the magnetization at 2 K both indicate the presence of long-range order within the complex. This was confirmed by the zero-field-cooled (ZFC) and field-cooled (FC) magnetizations in the 1.8–5 K temperature range (Figure 5). The ZFC/FC measurements were carried out at the very small field of 50 Oe for **1**. The two curves are superposed at the higher temperatures, increase sharply below 4 K, and then diverge at around 2.5 K. At a small field of 50 Oe, χ_m does not have a peak, indicating that the interaction between the chains is ferromagnetic. Although ferromagnetic interactions mediated by ligand L are rare and no other cases have been reported, a similar ligand, nicotinate *N*-oxide, enables the transfer of ferromagnetic interactions between metal ions.[13] The existence of ferromagnetic order was also confirmed by the field-dependent maximum of the $\chi_m T$ curve at low temperature (Figure S3) and by the fact that the saturation effect was present even at the very small field of 50 Oe. To further probe the long-range ordering in **1**, alternating current (AC) magnetic susceptibility measurements were performed in a field of 3.5 Oe, which oscillated at different AC frequencies. These measurements indicated that a magnetic phase transition occurred below 3 K, because both in-phase χ_m' and out-of-phase χ_m'' were observed around this temperature (Figure 5b). The fact that both the in-phase χ_m' and the out-of-phase χ_m'' are frequency-dependent indicates that **1** exhibits the spin glass state below 2.5 K. The frequency shift parameter, $\Phi = \Delta T_p / [T_p \Delta(\log f)] = 0.05$, is in the range of glass behavior.[14] The relaxation time was obtained from the Arrhenius-type equation $\tau(T) = \tau_0 \exp(-\Delta/kBT)$, where $\tau_0 = 1.13 \times 10^{-25}$ s and Δ/kB = 118.69 K (Figure 5b inset). This spin glass state is probably due to some defects in the crystal that lead to competition between the ferromagnetic and the antiferromagnetic interactions. Though there is no cusp in the χ_m vs. T curve at low temperature, even when a very small field of 50 Oe is used (Figure 5), if a cusp exists it may be at least at a point lower then 2 K. These interactions are mediated by the methoxy and *syn*,*syn* carboxylate groups, respectively, in the chains. No significant hysteresis was observed in **1** at 2 K (Figure 5a, inset), which agrees with the soft magnetic behavior described for **1**.

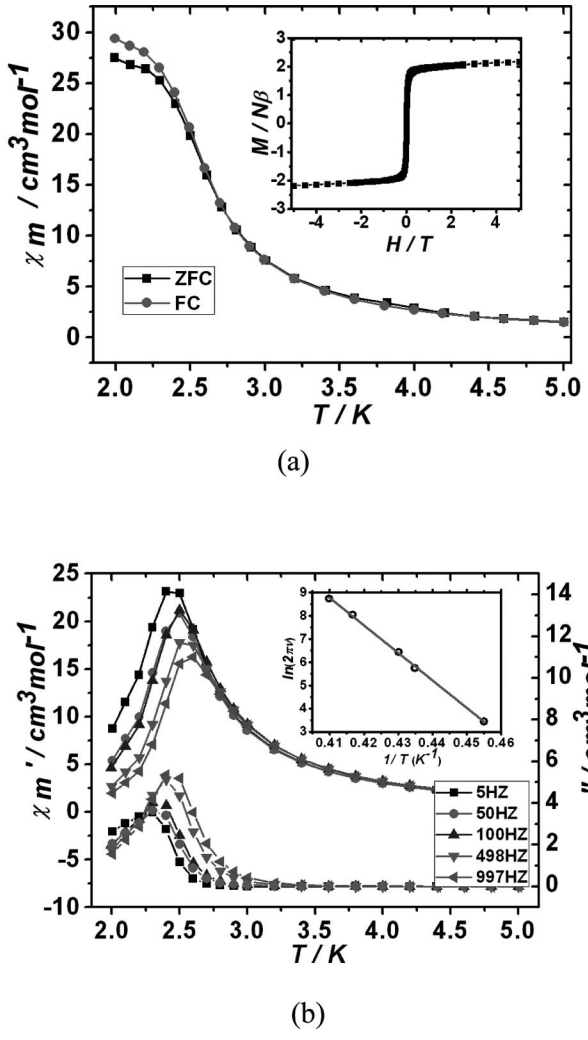

Figure 5. (a) ZFC and FC curves for **1**. Inset: the hysteresis for **1** at 2 K. (b) AC magnetic susceptibility plot at different frequencies for **1**. Inset: the fitting of the relaxation time to an Arrhenius-type equation.

The magnetic susceptibilities of **2** were explored at 2 kOe and are shown as a $\chi_m T$ vs. T plot in Figure 6a. The $\chi_m T$ value per formula unit for **2** decreases smoothly from 9.36 $cm^3 K mol^{-1}$ with the decrease in temperature from 300 to 100 K. However, when the temperature drops below 100 K, the $\chi_m T$ value decreases sharply to 1.31 $cm^3 K mol^{-1}$ at 2 K. Fitting the data between 30 and 300 K to the Curie–Weiss equation gives C = 10.07 $cm^3 K mol^{-1}$, θ = –19.14 K (Figure 6a). The C value is consistent with the value of three non-interacting Co^{II} ions with spin–orbit coupling, given g = 2.3–2.7. The temperature-dependent behavior of **2**

can be attributed to the synergy between the local magnetic effects (including the spin–orbit coupling ligand-field distortion) and the magnetic interactions between the Co^{II} ions.[15] In terms of magnetism, **2** exhibits alternating chains consisting of double azide-bridged trinuclear Co^{II} units. As with **1**, the data for **2** was fitted to the exponential equation over the full temperature range to give: C_1 = 3.2 $cm^3\,K\,mol^{-1}$, C_2 = 7.06 $cm^3\,K\,mol^{-1}$, αJ = –69.13 K, and βJ = –4.38 K. The negative values for αJ and βJ correspond to the spin–orbit coupling and the overall antiferromagnetic exchange interactions within the chain.[11d,16] In terms of the magnetic chain of **2**, the interactions mediated by the *syn*,*syn*-carboxylate and the double end-on azide ligands between Co1 and Co2 should be ferromagnetic,[7,15,16,17] whereas the interactions between two trinuclear units should be antiferromagnetic.[18] Accordingly, an -AFM-FM-FM- coupling sequence exists and leads to a nonmagnetic ground state (-↓ ↓ ↓ ↑ ↑ ↑ -) in the chain. The spin–orbit coupling effects and the -AFM-FM-FM- coupling affect the $\chi_m T$ vs. T values throughout the temperature range. The antiferromagnetic ground state of **2** is further supported by the fact that the magnetization (2.9 $N\beta$ per formula unit or 0.97 $N\beta$ per Co atom) at 5 T is much lower than expected (2–3 $N\beta$ per Co atom).

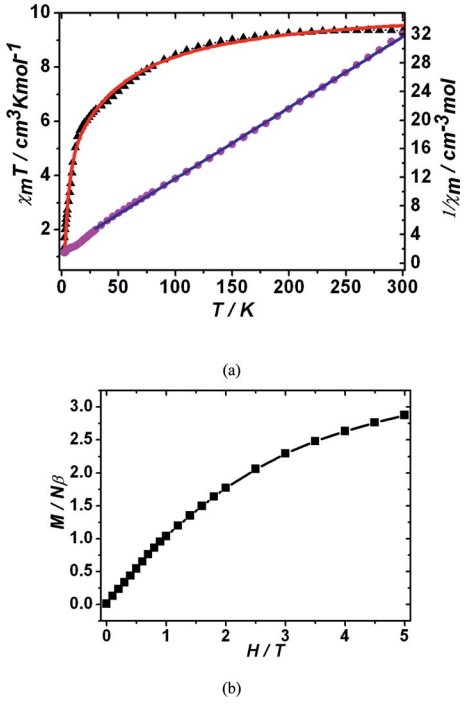

Figure 6. (a) Thermal variation of $\chi_m T$ and Curie plot for **2**. The solid line represents the best fit for the data where red is the exponential fit and blue is the fit to the Curie–Weiss equation. (b) Magnetization for **2** at 2 K.

Conclusions

Two new cobalt isonicotinate *N*-oxide complexes, **1** and **2**, containing short bridging methoxy or azide ligands, were synthesized. In **1** and **2** the isonicotinate *N*-oxide ligands all adopt the μ-4 bridging mode with the *syn*,*syn*-carboxylate and the μ-2-*N*-oxide groups. Complex **1** has a 3D structure containing an *N*-oxide/carboxylate/methoxy mixed-bridged Co^{II} 1D chain. Ferromagnetic couplings are found both within and between the chains, and **1** exhibits a spin glass state below 2.5 K. Complex **2** has a 2D structure based on a double end-on azido-bridged trinuclear Co^{II} unit. Ferromagnetic coupling exists in the trinuclear unit but antiferromagnetic interaction was found between the trinuclear units. This leads to an antiferromagnetic ground state in **2**.

Experimental Section

Materials and Physical Measurements

All the chemicals used for synthesis are of analytical grade and commercially available. Isonicotinate *N*-oxide acid, formic acid, cobalt carbonate, and methanol were purchased from commercial sources and used as received. $Co(HCO_2)_2{\cdot}4H_2O$ was synthesized by dissolving cobalt carbonate in formic acid and concentrating the solution. The solid product was separated by filtration.

Elemental analyses (C, H, N) were performed with a Perkin–Elmer 240C elemental analyzer. IR spectra were measured with a Tensor 27 OPUS (Bruker) FTIR spectrometer with KBr pellets. X-ray powder diffraction (XRPD) spectra were recorded with a Rigaku D/Max-2500 diffractometer at 50 kV, 40 mA for a Cu-target tube and a graphite monochromator. Simulation of the XRPD spectra was carried out with the single-crystal data and the diffraction-crystal module of the Mercury (Hg) program available free of charge via the Internet (http://www.iucr.org).

Magnetic data were collected by using crushed crystals of the samples with a Quantum Design MPMS-XL SQUID magnetometer equipped with a 5 T magnet. The data were corrected by using Pascal's constants to calculate the diamagnetic susceptibility, and an experimental correction for the sample holder was applied.

$[Co(OCH_3)L]_n$ (1): A mixture of $Co(HCO_2)_2{\cdot}4H_2O$ (1 mmol) and HL (L = isonicotinate *N*-oxide) (0.75 mmol) in methanol (15 mL) was sealed in a Teflon-lined stainless steel vessel, heated at 140 °C for 2 d under autogenous pressure, and then cooled to room temperature. Brown crystals of **1** were isolated in approximately 20% yield based on HL. FTIR (KBr pellets): $\tilde{\nu}$ = 3036, 2904, 2800, 2557, 1615, 1501, 1396, 1197, 1147, 1050, 889, 866, 812, 782, 686, 648, 513, 460 cm^{-1}. $C_7H_7CoNO_4$ (228.07): calcd. C 36.86, H 3.09, N 6.14; found C 36.58, H 3.10, N 6.28.

$[Co_3(N_3)_4L_2(HOCH_3)_2]_n$ (2): A mixture of $Co(NO_3){\cdot}6H_2O$ (1.5 mmol), sodium azide (2.0 mmol), and HL (0.75 mmol) in methanol (15 mL) was sealed in a Teflon-lined stainless steel vessel, heated at 100 °C for 2 d under autogenous pressure, and then cooled to room temperature. Mauve crystals of **2** were isolated in approximately 20% yield based on HL. FTIR (KBr pellets): $\tilde{\nu}$ = 3125, 2360, 1627, 1597, 1570, 1402, 1293, 1223, 1126, 1026, 947, 806, 770, 670, 449 cm^{-1}. $C_{14}H_{16}Co_3N_{14}O_8$ (685.17): calcd. C 24.54, H 2.35, N 28.62; found C 24.69, H 2.53, N 28.94.

X-ray Data Collection and Structure Determination: X-ray single-crystal diffraction data for **1** and **2** were collected with a Rigaku SCX-mini diffractometer at 293(2) K with Mo-K_α radiation (λ = 0.71073 Å) by using the ω-scan mode. The program SAINT[19] was used for integration of the diffraction profiles. All the structures were solved by direct methods using the SHELXS program of the SHELXTL package and refined by full-matrix least-squares meth-

ods with SHELXL (semi-empirical absorption corrections were applied using the SADABS program).[20] The metal atoms in each complex were located from the *E*-maps, and other non-hydrogen atoms were located during successive difference Fourier syntheses and refined with anisotropic thermal parameters on F^2. The hydrogen atoms of the ligands were generated theoretically on the specific atoms and refined isotropically with fixed thermal factors. Detailed crystallographic data are summarized in Table 2.

Table 2. Crystal data and structure refinement parameters for complexes **1** and **2**.

	1	**2**
Chemical formula	$C_7H_7CoNO_4$	$C_{14}H_{16}Co_3N_{14}O_8$
Formula weight	228.07	685.17
Space group	*Pnma*	$P\bar{1}$
a /Å	17.115(3)	8.7124(17)
b /Å	6.2802(13)	8.8764(18)
c /Å	7.5309(15)	9.0999(18)
α /°	90	107.14(3)
β /°	90	113.61(3)
γ /°	90	100.43(3)
V /Å^3	809.5(3)	579.1(2)
Z	4	1
D /g cm^{-3}	1.871	1.965
μ /mm^{-1}	2.097	2.199
T /K	293(2)	293(2)
R_1[a]/wR_2[b]	0.0479/0.0942	0.0774/0.1529

[a] $R_1 = \Sigma||F_o| - |F_c||/\Sigma|F_o|$. [b] $wR_2 = \{\Sigma[w(F_o^2 - F_c^2)^2]/\Sigma w(F_o^2)^2\}^{1/2}$.

CCDC-764137 (for **1**) and -764138 (for **2**) contain the supplementary crystallographic data for this paper. These data can be obtained free of charge from The Cambridge Crystallographic Data Center via www.ccdc.cam.ac.uk/data_request/cif.

Supporting Information (see footnote on the first page of this article): XRPD spectra for **1** and **2**, and curves of $\chi_m T$ versus *T* for **1**.

Acknowledgments

This work was supported by the National Natural Science Foundation of China (Nos. 20801041 and 20771082).

[1] M. Kurmoo, *Chem. Soc. Rev.* **2009**, *38*, 1353–1579.
[2] A. P. B. Lever, *Inorganic Electronic Spectroscopy*, Elsevier, Amsterdam, **1986**.
[3] J. B. Goodenough, J. S. Griffith, *The Theory of Transition-Metal Ions*, Cambridge University Press, **1964**.
[4] J. S. Griffith, *Phys. Rev.* **1968**, *171*, 466–479.
[5] a) H.-P. Jia, W. Li, Z.-F. Ju, J. Zhang, *Eur. J. Inorg. Chem.* **2006**, 4264–4270; b) D. Ghoshal, G. Mostafa, T.-K. Maji, E. Zangrando, T.-H. Lu, J. Ribas, N. R. Chaudhuri, *New J. Chem.* **2004**, *28*, 1204–1213.
[6] a) J. B. Goodenough, *Magnetism and Chemical Bonds*, Wiley-Interscience, New York, **1963**; b) T.-F. Liu, D. Fu, S. Gao, Y.-Z. Zhang, H.-L. Sun, G. Su, Y.-J. Liu, *J. Am. Chem. Soc.* **2003**, *125*, 13976–13977; c) S.-Q. Bai, E.-Q. Gao, Z. He, C.-J. Fanga, C.-H. Yan, *New J. Chem.* **2005**, *29*, 935–941.
[7] a) Y. Nishida, S. J. Kida, *J. Chem. Soc., Dalton Trans.* **1986**, 2633–2640; b) V. McKee, M. Zvagulis, C. A. Reed, *Inorg. Chem.* **1983**, *22*, 2914–2919; c) V. McKee, M. Zvagulis, J. V. Dagdigian, M. G. Match, C. A. Reed, *J. Am. Chem. Soc.* **1984**, *106*, 4765–4772.
[8] a) Y.-H. Zhao, H.-B. Xu, Y.-M. Fu, K.-Z. Shao, S.-Y. Yang, Z.-M. Su, X.-R. Hao, D.-X. Zhu, E.-B. Wang, *Cryst. Growth Des.* **2008**, *8*, 3566–3576; b) Z. He, Z.-M. Wang, S. Gao, C.-H. Yan, *Inorg. Chem.* **2006**, *45*, 6694–6705.
[9] F. E. Mabbs, D. J. Machin, *Magnetism and Transition Metal Complexes*, Chapman and Hall, London, **1973**.
[10] a) F. Lloret, M. Julve, J. Cano, R. Ruiz-García, E. Pardo, *Inorg. Chim. Acta* **2008**, *361*, 3432–3445; b) MAGPACK Program: J. J. Borrás-Almenar, J. M. Clemente-Juan, E. Coronado, B. S. Tsukerblat, *J. Comput. Chem.* **2001**, *22*, 985–991 and references cited therein.
[11] a) J.-M. Rueff, N. Masciocchi, P. Rabu, A. Sironi, A. Skoulios, *Eur. J. Inorg. Chem.* **2001**, 2843–2848; b) J.-M. Rueff, N. Masciocchi, P. Rabu, A. Sironi, A. Skoulios, *Chem. Eur. J.* **2002**, *8*, 1813–1820; c) M. Drillon, P. Panissod, P. Rabu, J. Souletie, V. Ksenofontov, P. Gütlich, *Phys. Rev. B* **2002**, *65*, 104404–104408; d) J. Souletie, P. Rabu, M. Drillon in *Scaling Theory Applied to Low Dimensional Magnetic System in Magnetism: Molecules to Materials* (Eds.: J. S. Miller, M. Drillon), Wiley-VCH, Weinheim, Germany, **2005**, vol. V, pp. 347–377.
[12] a) R. L. Carlin, *Magnetochemistry*, Springer-Verlag, Berlin, **1986**; b) H. S. Yoo, J. Kim II, N. Yang, E. K. Koh, J.-G. Park, C. S. Hong, *Inorg. Chem.* **2007**, *46*, 9054–9056; c) M. E. Lines, *J. Chem. Phys.* **1971**, *55*, 2977–2984.
[13] J.-P. Zhao, B.-W. Hu, Q. Yang, T.-L. Hu, X.-H. Bu, *Inorg. Chem.* **2009**, *48*, 7111–7116.
[14] a) A. H. Morrish, *The Physical Principles of Magnetism*, Wiley, New York, **1966**; b) J. A. Mydosh, *Spin Glasses: An Experimental Introduction*, Taylor & Francis, London, **1993**.
[15] Y. Ma, J.-Y. Zhang, A.-L. Cheng, Q. Sun, E.-Q. Gao, C.-M. Liu, *Inorg. Chem.* **2009**, *48*, 6142–6151.
[16] F.-C. Liu, Y.-F. Zeng, J. Jiao, X.-H. Bu, J. Ribas, S. R. Batten, *Inorg. Chem.* **2006**, *45*, 2776–2778.
[17] a) T. Liu, Y.-J. Zhang, Z.-M. Wang, S. Gao, *Inorg. Chem.* **2006**, *45*, 2782–2784; b) J. Ribas, A. Escuer, M. Monfort, R. Vicente, R. Cortés, L. Lezama, T. Rojo, *Coord. Chem. Rev.* **1999**, *193–195*, 1027–1068 and references cited therein.
[18] a) O. Fabelo, L. Cñadillas-Delgado, J. Pasán, F. S. Delgado, F. Lloret, J. Cano, M. Julve, C. Ruiz-Pérez, *Inorg. Chem.* **2009**, *48*, 11342–11351; b) O. Fabelo, J. Pasán, L. Cñadillas-Delgado, F. S. Delgado, F. Lloret, M. Julve, C. Ruiz-Pérez, *Inorg. Chem.* **2009**, *48*, 6086–6095.
[19] Bruker AXS, *SAINT Software Reference Manual*, Madison, WI, **1998**.
[20] a) G. M. Sheldrick, *SADABS*, *Siemens Area Detector Absorption Corrected Software*, University of Göttingen, Germany, **1996**; b) G. M. Sheldrick, *SHELXTL NT Version 5.1. Program for Solution and Refinement of Crystal Structures*, University of Göttingen, Germany, **1997**.

Received: February 26, 2010
Published Online: August 16, 2010

